PUBLISHED ONLINE: 29 JUNE 2009 | DOI: 10.1038/NPHOTON.2009.111

Plasmonics for near-field nano-imaging and superlensing

Satoshi Kawata[1,2], Yasushi Inouye[3] and Prabhat Verma[1,3]

Diffraction of light prevents optical microscopes from having spatial resolution beyond a value comparable to the wavelength of the probing light. This essentially means that visible light cannot image nanomaterials. Here we review the mechanism for going beyond this diffraction limit and discuss how manipulation of light by means of surface plasmons propagating along the metal surface can help to achieve this. The interesting behaviour of light under the influence of plasmons not only allows superlensing, in which perfect imaging is possible through a flat thin metal film, but can also provide nano-imaging of practical samples by using a localized surface plasmon mode at the tip of a metallic nanoprobe. We also discuss the current research status and some intriguing future possibilities.

Scientists have long dreamt of an optical microscope that can be used to see a sample in nanometre resolution. Because light propagates through water and air, an optical microscope can be used to see, *in vivo*, the details of living matter and other materials in their unperturbed natural condition. In addition, an optical microscope provides colour images that contain much richer information than other microscopes in which only monochrome images are produced. In particular, the visible and mid-infrared region of light covers the energies corresponding to the electronic transitions in atoms and to molecular vibrations, allowing optical microscopes to provide information related to the intrinsic properties of the sample. But the resolution attainable with an optical microscope is limited to about 0.5 μm because of the diffraction of light[1–3]. Therefore, it becomes almost impossible to image a sample at the nanoscale through an optical microscope.

Breaking through this limit, an optical microscope was proposed in which a nano-sized metallic probe tip scans the sample surface to form an image with a resolution much better than the diffraction limit[4]. The mechanism is based on the excitation of localized modes of surface plasmon polaritons (SPP) at the metallic tip, which generates a nano-sized spot of light at the apex of the nano-tip. By using this tiny light-spot as the light source of an optical microscope, extremely high spatial resolution can be obtained. The fundamental idea of exciting SPP to obtain images beyond the diffraction limit of light has been used in other studies as well. For example, the perfect lens or superlens proposed by Pendry also images a sample in nanoscopic resolution by exciting SPP at its resonance frequency[5,6]. Here we review the mechanism of optical nano-imaging based on the excitation of SPP to provide spatial resolution beyond the diffraction limit. We discuss a variety of metallic nanostructures as probes and look at their applications.

Super-resolution imaging by slow light

According to Abbe's diffraction theory, the minimum separation Δx of two points that can be resolved in an image constructed through a lens based on Rayleigh's criterion is given by

$$\Delta x = \frac{0.61\lambda}{n \sin\theta} \qquad (1)$$

where λ is the wavelength of light, n is the refractive index of the medium, and 2θ is the angular aperture of the lens on the object side[7]. Here, the angular aperture and the refractive index are both physically limited. Thus the wavelength λ is the only parameter that can be manipulated to obtain a desired value of the spatial resolution. To obtain super-resolution, we need to shorten the wavelength. But at the same time, to stay in the visible or infrared region in order to image the intrinsic properties of a sample as shown by its electronic or vibrational energies, we must not change the frequency or the energy of the light.

The wavelength of light is inversely proportional to the angular frequency, ω, as $\lambda = 2\pi c/\omega$, where c is the speed of light. If one can reduce the speed of light while keeping the frequency constant, the wavelength of light can be shortened and hence a higher resolution obtained in an image. Classically, this has been done by filling the space between the lens and sample surface with some high-refractive-index material such as immersion oil. This method improves the resolution within the limits of available refractive indices (less than 2). In some cases, it is possible to increase the refractive index further, but then it is difficult to keep the medium transparent in the visible regime. For substantial improvement in spatial resolution, we need a different method for reducing the speed of light.

There exists a form of slow light on the surface of a metal that travels along the surface as an evanescent wave associated with the collective oscillations of free electrons. In quantum form, this is called the surface plasmon polariton, and we can take advantage of this for high-resolution imaging. Figure 1a shows a typical plot for the dispersion curves of SPP and light. The dispersion for the light shows a linear relationship between frequency (energy) and wavenumber (momentum) whereas the dispersion for the SPP shows a curve. As the frequency approaches the resonance of SPP, the SPP dispersion curve moves away from the light line with a gentle slope. That means that the wavelength of SPP is shortened and the speed decreases. The light line and the SPP line never cross each other, and hence there is a phase mismatch for all values of the frequency. This prevents any coupling between propagating light and SPP[8–12]. Note that above the plasmon frequencies, the metal becomes dielectric, and for lower frequencies in the terahertz region, plasmonic effects disappear. But if the light is slow, as is the case for evanescent light near the surface of a metal, the dispersion for light has a different angle, as illustrated in Fig. 1a, and hence it crosses the SPP line at a certain frequency. This essentially means that there can be a coupling between the evanescent light and SPP at this particular frequency, resulting in resonant excitation of SPP.

The use of SPP on a gold thin film for subwavelength imaging was demonstrated by Smolyaninov *et al.*, who used a 502-nm line of an argon-ion laser to excite the SPP[8]. The authors put a small droplet of glycerin on a gold film, the parabolic boundary of which worked

[1]Department of Applied Physics, Osaka University, Suita 565-0871, Osaka, Japan. [2]RIKEN, Wako, Saitama 351-0198, Japan. [3]Graduate School of Frontier Biosciences, Osaka University, Suita 565-0871, Osaka, Japan. e-mail: kawata@ap.eng.osaka-u.ac.jp; verma@ap.eng.osaka-u.ac.jp

as a magnifying mirror in two dimensions (2D). A sample was set on the gold film under the glycerin droplet, and a magnified image formed by the glycerin droplet was observed through an ordinary microscope, as illustrated in Fig. 1b. Periodic nanohole arrays are ideal test samples in this demonstration, because when they are illuminated by laser light, they produce propagating surface waves, explaining the anomalous transmission of such an array at optical frequencies. The authors therefore selected a suitably designed periodic nanohole array as the sample. The SPP wavelength of gold excited by light at 502 nm corresponds to ~70 nm, resulting in resolution enhancement by a factor of ~7. This demonstration can be considered as a kind of plasmon microscope in 2D. Near-field light cannot be detected in the far field, so such a microscope must include a mechanism that can convert the near field into far field. Roughness, protrusion or periodic corrugation on the metal surface can do this job by coupling SPP out to the far field[9–12].

Superlens as an extreme case

In the extreme case, as the angular frequency ω approaches the resonance frequency ω_{sp}, the wavenumber k_{sp} associated with SPP goes to infinity, which means the speed goes down to zero. This is the case of the superlens[5] which permits perfect imaging through a metal film (made from a noble metal such as gold or silver) without any blurring. In ref. 5, and in several other articles[13–17], the superlens phenomenon is primarily explained through negative refraction, but an analogous way to understand it is to consider the slowing of light at metallic surfaces.

Imaging through a superlens essentially requires both the object and the image to be within the near-field range. Therefore, it becomes impossible to read the image through a conventional optical system with a lens or a mirror. Instead, Zhang and his group recorded the near-field image on photoresist and read it by atomic force microscopy (AFM)[17]. Figure 2 explains their experiment and results. An object in the form of the word 'NANO' was imaged on a photoresist through a 35-nm-thick silver film that acted as the superlens. A resolution of about 65 nm was obtained. A superlens with magnifying function was later proposed by several authors[18–21] independently, with either a cylindrical geometry for the silver film or a tapered arrangement of silver nanorods.

A superlens has some practical limits in obtaining high resolution. In addition to questions of structural quality such as surface roughness and purity of material against oxidization and/or sulphurization, the absorption of plasmons in metal is an essential limitation. The imaginary part of the dielectric constant of a metal is not negligible, and plasmon resonance typically decays with a half-life of a few picoseconds or less. This causes loss of information and hence blurring of the image.

Metallic tip for nano-imaging

Although a superlens can provide an image of nanostructure well beyond the diffraction limit, a large, flat metallic surface restricts the geometry of the sample for practical imaging. If the metal structure can be made much smaller than the wavelength of propagating light, one can scan such a nanostructure along the sample surface as a probe, similar to the other scanning probe microscopes[22], and image a sample with high resolution geometry. The SPP of a metallic nanoparticle is strongly localized and hence the dispersion relation is different from the one shown in Fig. 1. Unlike the SPP of a large metallic structure, the localized modes of SPP in a small metallic structure can couple with the propagating photons, which essentially means slowing down of the light or reduction in the effective wavelength close to the metallic nanostructure. The advantage of this system is that, owing to the small size of the metallic structure, there is no propagation of SPP, and hence losses related to the retardation of SPP do not exist. Any microscopy involving this confined light field will therefore have a spatial

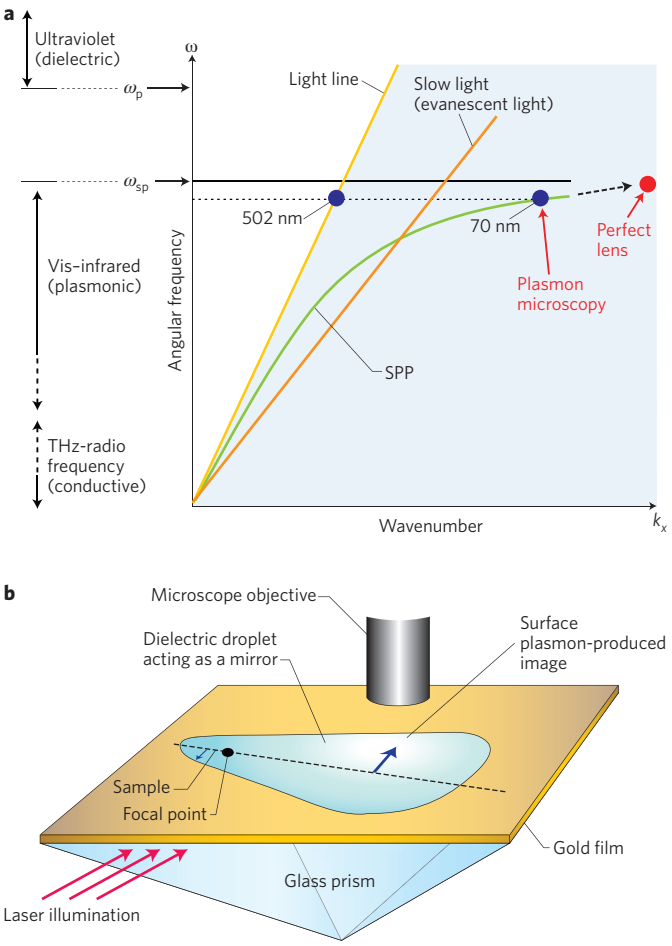

Figure 1 | Slow light on metal surface. a, Dispersion relation of propagating light, evanescent light and SPP. The blue circles show that propagating light with a wavelength of 502 nm can excite SPP with a wavelength of 70 nm in the plasmon microscopy demonstrated in ref. 8. The red circle indicates the ideal case of a perfect lens. **b**, Geometry of 2D plasmon microscopy. The structure on the metal surface is magnified by the parabolic boundary of a dielectric droplet that works as a mirror, and the image is detected through an ordinary objective lens. Reproduced with permission from ref. 8. © 2005 OSA.

resolution comparable to the size of the confined field, which is the same as the size of the metallic nanostructure. The metallic structure could be a nanosphere, a nanorod, a nanocone or other shape[23–25].

Figure 3 shows some examples of metallic nanoscale tips used as the probe in this imaging technique. A numerical simulation (Fig. 3a) shows the confinement of light at the apex of a tip. The tip can be scanned over a sample, as in Fig. 3b, to construct an image. Several methods for preparing metallic nano-tips have been proposed, as illustrated in Fig. 3c–e: for example, an AFM cantilever tip could be coated with a thin silver film[26], a silver or gold nanoparticle could be attached to the end of a pointed optical fibre[27,28] or a silver wire could be electrochemically etched after milling with a focused ion beam[29].

This concept was first demonstrated by Kawata's group through an apertureless near-field scanning optical microscope (NSOM) in 1994, where a metallic scanning tunnelling microscope (STM) tip, illuminated with evanescent light, was scanned over the sample[4]. Boccara and his group[30] reported the same concept in 1995 for infrared imaging, using a bent conical tungsten tip as an apertureless NSOM probe. During the same period, Wickramasinghe's group reported apertureless NSOM with a non-metallic silicon tip[31], where

NATURE PHOTONICS DOI: 10.1038/NPHOTON.2009.111

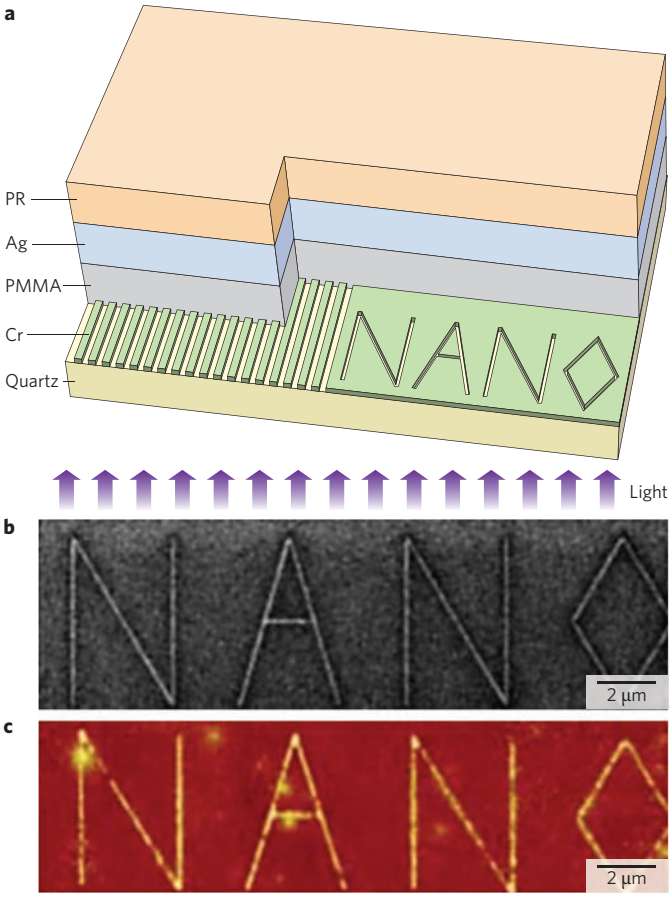

Figure 2 | Experimental demonstration of subwavelength imaging through a thin silver layer. a, An illustration of experimental demonstration of subwavelength imaging through a superlens. The sample, inscribed in the form of the word 'NANO' in chromium film, is separated by a thin layer of polymethyl methacrylate (PMMA) from a 35-nm-thick silver film acting as a superlens. The image is recorded on a photoresist in the form of topographic modulation. **b**, A focused ion beam (FIB) image of the inscribed object. **c**, AFM image of the topographic modulation corresponding to the near-field image obtained from the superlens. Images in **a**, **b** and **c** are reproduced with permission from ref. 17. © 2005 AAAS.

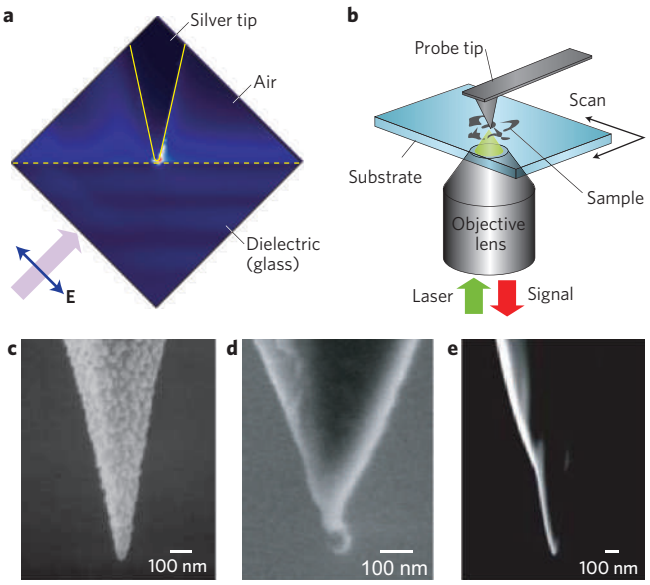

Figure 3 | Commonly used metallic nanoprobes. a, Numerical calculation of light distribution at the apex of a metallic nano-tip shows an enhancement of ~100 times[41]. **b**, A typical set-up for apertureless NSOM, where a nano-tip is illuminated through a thin sample and the signal is collected by the same objective lens that illuminates the tip. Image is obtained by scanning the sample stage. **c**–**e**, Scanning electron microscope images of some commonly used metallic nano-tips. **c**, Cantilever coated with silver thin film by evaporation. **d**, Gold nanoparticle attached to pointed optical fibre. **e**, Electrochemically etched silver wire. Images in **c**, **d** and **e** reproduced with permission from, respectively, ref. 26. © 2001 Elsevier; ref. 28. © 2006 APS; and ref. 29. © 2003 APS.

there were no involvements of plasmons. Rather, interferometric detection was used to measure the local refractive index for imaging. Knoll and Keilmann used interferometry for infrared imaging[32], and there have been several other reports[33] on similar research. In the infrared region, because the dispersion curve of SPP for metal approaches the light line (Fig. 1), SPP-assisted light enhancement is not expected.

In an interesting proposal for a NSOM probe, a tip was prepared by coating a metal thin film over a small protrusion on an otherwise flat surface, producing a localized field at the protrusion to sense the local dielectric constant of a sample[34]. In another study, a microscope was invented in which a gold nanoparticle trapped and controlled by a laser beam was used as an imaging probe[35]. By scanning such a trapped gold particle over the sample surface, an image of fluorescent DNA entangles was demonstrated.

In the early stage of near-field microscopy, apertured tips were used to confine the light by passing it through a tiny hole at the apex of the tip. Although this kind of NSOM has certain advantages, such as a reduction of far-field background or the potential to characterize a plasmonic device, it always suffers from comparatively low resolution that is governed by the size of the aperture.

Enhancement of confined light

In addition to high resolution, plasmonic nano-imaging is advantageous in terms of optical throughput. The field intensity near the metallic nanostructure is highly enhanced owing to the resonance of localized SPP. The enhancement factor strongly depends on the shape and the size of the metallic nanostructure. Figure 4a illustrates some of the nanostructures commonly used for this purpose. An easy way to understand the light–metal interaction for a nanostructure is to consider the separation of free charge carriers under the influence of the external electric field associated with the propagating light. This separation creates an additional field that oscillates with the same frequency as the external field. As a result, an extremely localized and enhanced light field is created close to the metal structure, as illustrated in Fig. 4a.

As plasmons tend to radiate at curvature, a spherical shape turns out not to be the best shape for enhancement. On the other hand, the formation of standing waves of SPP in a structure with appropriate geometry provides strong resonances and hence supports stronger enhancement[36,37]. In that sense, a rod with optimized aspect ratio seems to be the best deal. Both ends of a rod can have a strongly confined field, usually known as the 'hot spot'. The other interesting structures are triangles and cones, which, owing to their sharp edges, produce strong concentration of free charge carriers at the apex, resulting in a higher field enhancement near the apex. Both triangular[38–40] and conical[41] nanostructures have been shown to produce enormous field enhancement. Many groups have also theoretically calculated the field enhancement for different shapes of metallic nanoprobes. Figure 4b shows one such numerical simulation result for a nanorod that is 150 nm long and has a diameter of 20 nm. The light source is considered as a dipole (indicated by the double-headed arrow) 10 nm from one end of the nanorod, and a hot spot is

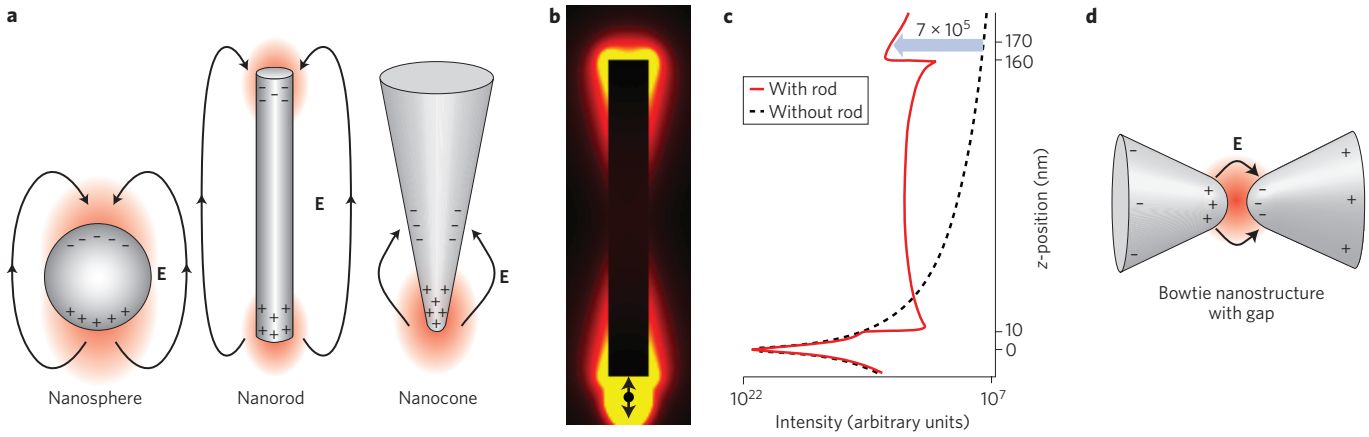

Figure 4 | Light field enhancement at metallic nanostructures. a, Illustration of some commonly used metallic nanostructures showing field enhancement. **b**, Simulation results showing the intensity distribution of the resonance mode of SPP along the cross-section of a 150-nm-long silver nanorod. **c**, The dashed line shows the natural decay of light intensity in the absence of the nanorod, and the red curve shows the intensity in the presence of the rod. A field enhancement of 7×10^5 can be realized. **d**, A bowtie-shaped nanostructure, which can have strong field enhancement within the nanogap.

observed at the other end. The colour distribution in Fig. 4b shows the light intensity distribution along the rod, and the red solid and black dashed curves in Fig. 4c show the intensity profiles along the length in the presence and absence of the rod, respectively. A comparison of the two curves reveals that the intensity enhancement at the end of the rod is a factor of about 10^6. Several researchers have made use of such a hot spot at the end of a nanorod to demonstrate considerable enhancement in Raman scattering[42–44].

When the SPP of one metallic nanostructure interacts with the SPP of another close by, the field enhancement at the nanogap between the two nanostructures can be many times larger[45,46]. This is illustrated in Fig. 4d, where field enhancement between two conical nanostructures arranged in the form of a bowtie[47–50] is depicted. Several research groups have studied enhancement at the nanogap between two metallic nanostructures for different kind of structures, including the plasmonic enhancement in surface-enhanced resonance spectroscopy (SERS)[51–57], where hot spots between nanostructures play an important part.

Tip-enhanced Raman and CARS imaging

As Raman spectroscopy provides information about molecular and lattice vibrations, one can observe the target directly without any need for staining or dye. Rich information is available from the vibrational modes, but owing to the second-order optical process involved in Raman scattering, the probability of the Raman process (typical cross-section 10^{-30} cm^2) is much smaller than that of infrared absorption (typical cross-section 10^{-20} cm^2) or fluorescence (typical cross-section 10^{-16} cm^2). Field enhancement can therefore make a useful contribution to Raman scattering, which has made SERS an important research topic, although SERS does not improve the spatial resolution. But if SERS is activated by a nanosized metallic structure instead of a large, rough metallic surface, one can achieve high resolution as well. The technique based on this phenomenon is called tip-enhanced Raman spectroscopy (TERS), where Raman scattering is combined with the NSOM technique. Between 1999 and 2000, three groups independently demonstrated the application of TERS[51,58,59]. Since then, plenty of nanomaterials have been investigated with TERS, examples being single-walled carbon nanotubes (SWNTs), fullerenes (C_{60}), DNA and strained silicon[29,60–68]. All these reports considered different kind of physical, chemical or even mechanical properties of samples at the nanoscale and pointed towards several interesting applications of TERS. Here we will review some of the well-known applications of plasmonic enhancement.

One of the common challenges in TERS is to achieve high spatial resolution. As an example of linear Raman scattering at high spatial resolution, we discuss the TERS imaging of SWNT reported in 2003 by Novotny's group[29]. The authors scanned a monodispersed SWNT sample at G′ Raman mode (2,615 cm^{-1}) to obtain a TERS image, which is shown in Fig. 5a. The spatial resolution of this image, as estimated from the line profile across the nanotubes (indicated by white dashed line), was 25 nm, which is about 25 times smaller than the wavelength of the excitation light (λ = 633 nm), showing extremely high spatial resolution. In later years, the same group showed even better spatial resolution, at about 35 times smaller than the probing wavelength[68].

Nonlinearity gives intrinsic confinement of photons in any nonlinear spectroscopy. Consequently, the spatial resolution of nanoimaging can be improved by combining the NSOM with nonlinear optical phenomenon. This was demonstrated by combining tip enhancement with coherent anti-Stokes Raman scattering (CARS)[61]. The sample was prepared by casting a network structure of double-stranded DNA consisting of adenine and thymine base pairs and a high-resolution tip-enhanced CARS (TE-CARS) image was obtained (Fig. 5b). The spatial resolution, as estimated from the line profile along the dotted line, was about 15 nm, which is about 60 times smaller than the probing wavelength (λ = 880 nm). This spatial resolution is almost a factor of 2 better than linear TERS. Apart from the resolution, the researchers also demonstrated, by imaging the diameter distribution in a bundle of SWNTs[69], that TERS imaging can reveal the distribution of intrinsic properties of a sample by means of coded colours.

Fluorescence imaging

Fluorescence microscopy also benefits from the confinement and enhancement of the light at the tip apex. In the early days of near-field optical imaging, Xie's group demonstrated a near-field two-photon excited fluorescence image by using a gold nano-tip and a mode-locked Ti:sapphire laser[70]. The group produced a tip-enhanced fluorescence image of a photosynthetic membrane fragment with spatial resolution of the order of 20 nm. Later, many other researchers achieved high-resolution fluorescence measurements by using the technique of field enhancement at a metallic nanostructure[71–76]. Recently, there has been a report on single molecular detection based on a similar concept[77]. One important drawback of tip-enhanced fluorescence is that the fluorescence tends to quench at the metallic tip, when the tip comes in close contact with the sample. The measured intensity of fluorescence is therefore a trade-off

NATURE PHOTONICS DOI: 10.1038/NPHOTON.2009.111

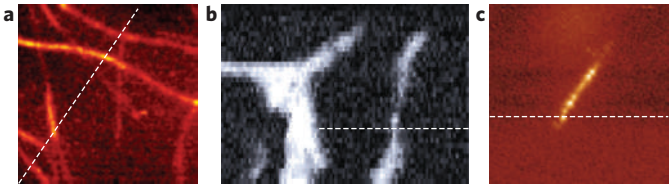

Figure 5 | High-resolution imaging through tip-enhancement effects. **a**, TERS image of SWNTs showing a spatial resolution of about 25 nm. **b**, TE-CARS image of a DNA network, with a spatial resolution better than 15 nm. The spatial resolution in Raman measurements can be improved by the nonlinearity in spectroscopy. **c**, Fluorescence image of an isolated SWNT, indicating a spatial resolution better than 15 nm. Images in **a**, **b** and **c** reproduced with permission from, respectively, ref. 29, © 2003 APS; ref. 61, © 2004 APS; and ref. 79, © 2005 ACS.

between quenching and enhancement[28,78]. Nevertheless, the results of fluorescence imaging through metallic tip have so far been outstanding. Figure 5c shows a tip-enhanced fluorescence image of SWNT, which is taken from the work of Novotny and his group[79]. A line profile corresponding to the dotted line in Fig. 5c determines the spatial resolution of the fluorescence image, which was found to be about 15 nm. Even though quenching is a serious obstacle, near-field fluorescence imaging has so far given us some important and interesting results. Recently, ion pump proteins bound in plasma membrane have been imaged in an aqueous environment by tip-enhanced fluorescent measurement[80,81]. Although the results of fluorescence enhancement near a metallic tip are evident, one should note that this technique suffers from bleaching over a long measurement time, particularly because the sample is illuminated over a much larger area than the actual measurement area. In contrast, similar Raman measurements do not have any bleaching.

Single-molecule detection

Even though Raman efficiency is extremely low, several researchers have demonstrated in the past decade that plasmonic enhancement (sometimes combined with chemical enhancement) in SERS can reveal the spectroscopic signature of a single molecule. In most of the studies, silver colloids mixed with Raman active molecules are immobilized on a suitable substrate[42,57,82,83]. The concentration of the molecule is usually chosen to be very low so that statistically there is no more than one molecule per colloid, and thus any Raman signal originating from the sample can be considered to be coming from a single molecule. The other signature considered to be a characteristic of single-molecule emission is strong temporal fluctuation of these SERS signals, both in intensity and spectral shape[57,82,83]. The general consensus is that there are very few active colloids capable of producing the hot spot for single-molecule detection. Although some researchers have suggested that these hot spots could be generated near a single isolated metal nanoparticle, most other researchers have found that the hot spots are typically at the junction between two or more closely spaced nanoparticles. Such an interpretation is also supported by theoretical studies[84,85].

Kneipp *et al.* demonstrated in 1997 that by using aggregated colloidal silver they could detect single molecules of crystal violet in near-infrared experiments[56]. In the same year, Nie and Emory demonstrated wonderful single-molecule SERS observations with visible light (λ = 514.5 nm) for rhodamine 6G molecules adsorbed on isolated silver nanoparticles[42]. Apart from Raman scattering, plasmonic enhancement was also used around the same time in other techniques, such as second harmonic generation, for field localization[86] and for the detection of single molecules[87]. Since then, many other reports have emerged on single-molecule detection through SERS[57,88–93], most of which discussed the importance of creating

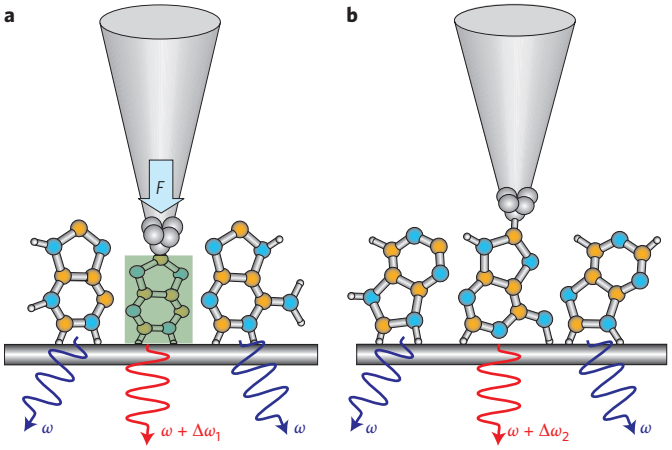

Figure 6 | Higher resolution in TERS through mechanical and chemical effects. **a**, When a sample is pressurized by a sharp tip during TERS measurement, selected sample molecules directly in contact with the tip apex can be compressed (coloured area). By sensing the modified vibrational frequencies of these molecules, one can achieve higher resolution. **b**, When the metallic tip comes into contact with a sample, some of the sample molecules may be adsorbed on the tip and change their orientations. This results in modified spectral response from these molecules, which can also provide very high spatial resolution, ideally to molecular level.

hot spots or boosting the surface active sites for better chemical enhancement. More recently, Le Ru *et al.* claimed that single-molecule observation is easier and more convincing when two dye molecules are mixed together[94].

Imaging beyond plasmonics

So far in this review, we have mainly discussed the interaction between light and local plasmons of a metallic nanostructure, which invokes some interesting phenomena in optical investigation of materials. The role of plasmonics in optical imaging is remarkable, as it takes us far beyond the conventional limits of spatial resolution in optical imaging. But we still come to a resolution limit of around 10–15 nm, beyond which it seems impossible to go solely with plasmonic effects. The limit of spatial resolution in plasmon-related optical observation essentially comes from the size of the metallic nanostructure used in plasmonic studies, because the volume of the confined light, which determines the spatial resolution, is comparable to the size of the metallic nanostructure. To obtain high spatial resolution, however, one cannot simply keep on decreasing the size of the metallic structure, because plasmons are quanta of 'collective' electron oscillation, and we need a number of metal atoms to have enough free electrons for their collective oscillation.

It is therefore necessary to think beyond plasmonic effects to reach even better spatial resolution than has been achieved in TERS experiments so far. A combination of TERS with a completely different phenomenon can potentially help TERS to achieve higher resolution. For example, by combining a nonlinear optical phenomenon with TERS, as discussed earlier, the spatial resolution in TE-CARS could be improved by almost a factor of 2 in comparison with linear TERS. More recently, it has been argued that a combination of mechanical effects with TERS has the potential to improve the spatial resolution much further[95]. In this technique, controlled pressure is applied on the sample by the tip. Owing to the small size of silver grains on the surface of the tip, the actual contact area between silver-coated tip and sample is only a few nanometres. The idea is based on the fact that when the sample is pressurized by the tip, only those sample molecules that are in contact with the silver grain would feel the pressure, resulting in a perturbed spectrum

with a different spectral shape, and hence could be distinguished from the rest of the sample molecules. The mechanism is illustrated in Fig. 6a, where the sample molecules directly under the tip apex are compressed, resulting in a modified frequency of vibration compared with the vibrations of other unpressurized molecules. By sensing this spectral change, it is possible to image the sample with a spatial resolution of a few nanometres, much better than the resolution achieved in simple TERS.

Another interesting phenomenon that can be combined with TERS for better spatial resolution is the chemical effect between the sample and the silver atoms on the tip apex. The large enhancement in SERS is partially attributed to chemical effects between the sample and the silver atoms[56,89–94]. TERS, however, can provide better control over chemical effects, because the distance between the tip and the sample can be precisely regulated[58,96,97]. Figure 6b illustrates that when a metallic tip is placed on the sample under precise control, only a few molecules are chemically adsorbed on the tip. These molecules would have a different spectral response from the other molecules, providing high spatial resolution, ideally to molecula level[98].

Future outlook

Although plasmonics has played an extremely important part in the area of nano-imaging by breaking through the conventional limits, we have come to realize that this phenomenon also has limitations on its spatial resolution. This primarily comes from the physical restrictions: for example, a certain minimum size of metallic nanostructure is required for efficient collective oscillation of plasmons. Thus going beyond plasmonics is a must for any further improvement. Although we have discussed some examples here, it will be crucial in the future to consider more physical phenomena that could be combined with plasmonics to improve the current limits. Another issue is spectroscopy with ultraviolet and deep-ultraviolet frequencies[99]. As seen in Fig. 1a, the plasmonic effect is significant only in the visible to near-infrared region. Noble metals including silver, gold and copper are not plasmonic beyond the plasmon resonance frequency, but dielectric. It will be essential to consider either natural or artificial materials that can work as plasmonic materials in this frequency region. Also, for frequencies lower than near-infrared, metals work as perfect conductors in which the wavelength shortening or slowing down of light is not observed. An artificial structure made by arranging conductive and dielectric layers can, however, show plasmonic behaviour in the terahertz (far infrared) to gigahertz (microwave) region[100]. Future research in this direction could prove to be decisive.

References

1. Abbe, E. Beiträge zur Theorie des Mikroskops und der mikroskopischen Wahrnehmung. *Arch. Mikroskop. Anat.* **9,** 413–420 (1873).
2. Sommerfeld, A. Ueber die Fortpflanzung elektrodynamischer Wellen laengs eines Drahtes. *Ann. Phys. Chem.* **303,** 233–290 (1899).
3. Heisenberg, W. Ueber den anschaulichen Inhalt der quantentheoretischen Kinematik und Mechanik. *Z. Phys.* **43,** 172–198 (1927).
4. Inouye, Y. & Kawata, S. Near-field scanning optical microscope with a metallic probe tip. *Opt. Lett.* **19,** 159–161 (1994).
5. Pendry, J. B. Negative refraction makes a perfect lens. *Phys. Rev. Lett.* **85,** 3966–3969 (2000).
6. Smith, D. R., Schurig, D., Rosenbluth, M. & Schultz, S. Limitations on subdiffraction imaging with a negative refractive index slab. *Appl. Phys. Lett.* **82,** 1506–1508 (2003).
7. Born, M. & Wolf, E. *Principles of Optics* (Pergamon, 1959).
8. Smolyaninov, I. I., Davis, C. C., Elliott, J. & Zayats, A. V. Resolution enhancement of a surface immersion microscope near the plasmon resonance. *Opt. Lett.* **30,** 382–384 (2005).
9. Raether, H. *Surface Plasmons* (Springer, 1998).
10. Bozhevolnyi, S. I., Vohnsen, B., Smolyaninov, I. I. & Zayats, A. V. Direct observation of surface polariton localization caused by surface roughness. *Opt. Commun.* **117,** 417–423 (1995).
11. Wood, R. W. On a remarkable case of uneven distribution of light in a diffraction grating spectrum. *Phil. Mag.* **4,** 396–402 (1902).
12. Kawata, S. *Near Field Optics and Surface Plasmon Polariton* (Springer, 2001).
13. Podolskiy, V. A. & Narimanov, E. E. Near-sighted superlens. *Opt. Lett.* **30,** 75–77 (2005).
14. Taubner, T., Korobkin, D., Urzhumov, Y., Shvets, G. & Hillenbrand, R. Near-field microscopy through a SiC superlens. *Science* **313,** 1595 (2006).
15. Fang, N. & Zhang, X. Imaging properties of metamaterial superlens. *Appl. Phys. Lett.* **82,** 161–163 (2003).
16. Rao, X. R. & Ong, K. C. Subwavelength imaging by a left-handed material superlens. *Phys. Rev. E* **68,** 067601 (2003).
17. Fang, N., Lee, H., Sun, C. & Zhang, X. Sub-diffraction-limited optical imaging with a silver superlens. *Science* **308,** 534–537 (2005).
18. Liu, Z., Lee, H., Xiong, Y., Sun, C. & Zhang, X. Far-field optical hyperlens magnifying sub-diffraction-limited optics. *Science* **315,** 1686 (2007).
19. Smolyaninov, I. I., Hung, Y. J. & Davis, C. C. Magnifying superlens in the visible frequency range. *Science* **315,** 1699–1701 (2007).
20. Shvets, G., Trendafilov, S., Pendry, J. B. & Sarychev, A. Guiding, focusing, and sensing on the subwavelength scale using metallic wire arrays. *Phys. Rev. Lett.* **99,** 53903 (2007).
21. Kawata, S., Ono, A. & Verma, P. Subwavelength colour imaging with a metallic nanolens. *Nature Photon.* **2,** 438–442 (2008).
22. Kawata. S. & Shalaev, V. M. *Tip-Enhancement* (Elsevier, 2007).
23. Link, S. & El-Sayed, M. A. Spectral properties and relaxation dynamics of surface plasmon electronic oscillations in gold and silver nanodots and nanorods. *J. Phys. Chem. B* **103,** 8410–8426 (1999).
24. Sun, Y. & Xia, Y. Shape-controlled synthesis of gold and silver nanoparticles. *Science* **298,** 2176–2179 (2002).
25. Prodan, E. M., Radloff, C., Halas, N. J. & Nordlander, P. A hybridization model for the plasmon response of complex nanostructures. *Science* **302,** 419–422 (2003).
26. Hayazawa, N., Inouye, Y., Sekkat, Z. & Kawata, S. Near-field Raman scattering enhanced by a metalized tip. *Chem. Phys. Lett.* **335,** 369–374 (2001).
27. Barsegova, I. *et al*. Controlled fabrication of silver or gold nanoparticle near-field optical atomic force probes: Enhancement of second-harmonic generation. *Appl. Phys. Lett*. **81,** 3461–3463 (2002).
28. Anger, P., Bharadwaj, P. & Novotny, L. Enhancement and quenching of single-molecule fluorescence. *Phys. Rev. Lett.* **96,** 113002 (2006).
29. Hartschuh, A., Sánchez, E. J., Xie, X. S. & Novotny, L. High-resolution near-field Raman microscopy of single-walled carbon nanotubes. *Phys. Rev. Lett.* **90,** 095503 (2003).
30. Gleyzes, P., Boccara, A. C. & Bachelot, R. Near field optical microscopy using a metallic vibrating tip. *Ultramicroscopy* **57,** 318–322 (1995).
31. Zenhausern, F., O'Boyle, M. P. & Wickramasinghe, H. K. Apertureless near-field optical microscope. *Appl. Phys. Lett*. **65,** 1623–1625 (1994).
32. Knoll, B. & Keilmann, F. Near-field probing of vibrational absorption for chemical microscopy. *Nature* **399,** 134–137 (1999).
33. Bachelot, R., Gleyzes, P. & Boccara, A. C. Near-field optical microscopy by local perturbation of a diffraction spot. *Microsc. Microanal. Microstruct.* **5,** 389–397 (1994).
34. Fischer, U. C. & Pohl, D. W. Observation of single-particle plasmons by near-field optical microscopy. *Phys. Rev. Lett.* **62,** 458–461 (1989).
35. Sugiura, T., Okada, T., Inouye, Y., Nakamura, O. & Kawata, S. Gold-bead scanning near-field optical microscope with laser-force position control. *Opt. Lett.* **22,** 1663–1665 (1997).
36. Krug, J. T. II, Sánchez, E. J. & Xie, X. S. Design of near-field optical probes with optimal field enhancement by finite difference time domain electromagnetic simulation. *J. Chem. Phys.* **116,** 10895–10901 (2002).
37. Martin, Y. C., Hamann, H. F. & Wickramasinghe, H. K. Strength of the electric field in apertureless near-field optical microscopy. *J. Appl. Phys.* **89,** 5774–5778 (2001).
38. Martin, O. J. F. & Girard, C. Controlling and tuning strong optical field gradient at a local probe microscope tip apex. *Appl. Phys. Lett*. **70,** 705–707 (1997).
39. Fischer, U. C., Koglin, J. & Fuchs, H. The tetrahedral tip as a probe for scanning near-field optical microscopy at 30 nm resolution. *J. Microsc.* **176,** 231–237 (1994).
40. Koglin, J., Fischer, U. C. & Fuchs, H. Material contrast in scanning near-field optical microscopy at 1–10 nm resolution. *Phys. Rev. B.* **55,** 7977–7984 (1997).
41. Furukawa, H. & Kawata, S. Local field enhancement with an apertureless near-field-microscope probe. *Opt. Commun.* **148,** 221–224 (1998).
42. Nie, S. & Emory, S. R. Probing single molecules and single nanoparticles by surface-enhanced Raman scattering. *Science* **275,** 1102–1106 (1997).
43. Kottmann, J. P., Martin, O. J. F., Smith, D. R. & Schultz, S. Dramatic localized electromagnetic enhancement in plasmon resonant nanowires. *Chem. Phys. Lett*. **341,** 1–6 (2001).

44. Tian, Z.-Q., Ren, B. & Wu, D.-Y. Surface-enhanced Raman scattering: From noble to transition metals and from rough surfaces to ordered nanostructures. *J. Phys. Chem. B.* **106,** 9463–9483 (2002).
45. Talley, C. E. *et al.* Surface-enhanced Raman scattering from individual Au nanoparticles and nanoparticle dimer substrates. *Nano Lett.* **5,** 1569–1574 (2005).
46. Su, K.-H. *et al.* Interparticle coupling effects on plasmon resonances of nanogold particles. *Nano Lett.* **3,** 1087–1090 (2003).
47. Farahani, J. N., Pohl, D. W., Eisler, H.-J. & Hecht, B. Single quantum dot coupled to a scanning optical antenna: a tunable superemitter. *Phys. Rev. Lett.* **95,** 17402 (2005).
48. Farahani, J. N. *et al.* Bow-tie optical antenna probes for single-emitter scanning near-field optical microscopy. *Nanotechnology* **18,** 125506 (2007).
49. Mühlschlegel, P., Eisler, H.-J., Martin, O. J. F., Hecht, B. & Pohl, D. W. Resonant optical antennas. *Science* **308,** 1607–1609 (2005).
50. Schuck, P. J., Fromm, D. P., Sundaramurthy, A., Kino, G. S. & Moerner, W. E. Improving the mismatch between light and nanoscale objects with gold bowtie nanoantennas. *Phys. Rev. Lett.* **94,** 017402 (2005).
51. Hayazawa, N., Inouye, Y., Sekkat, Z. & Kawata, S. Metallized tip amplification of near-field Raman scattering. *Opt. Commun.* **183,** 333–336 (2000).
52. Pettinger, B., Ren, B., Picardi, G., Schuster, R. & Etrl, G. Nanoscale probing of adsorbed species by tip-enhanced Raman spectroscopy. *Phys. Rev. Lett.* **92,** 096101 (2004).
53. Futamata, M., Maruyama, Y. & Ishikawa, M. Critical importance of the junction in touching Ag particles for single molecule sensitivity in SERS. *J. Mol. Struct.* **735,** 75–84 (2005).
54. Hao, F. & Nordlander, P. Plasmonic coupling between a metallic nanosphere and a thin metallic wire. *Appl. Phys. Lett.* **89,** 103101 (2006).
55. Le, F., Lwin, N. Z., Halas, N. J. & Nordlander, P. Plasmonic interactions between a metallic nanoshell and a thin metallic film. *Phys. Rev. B* **76,** 165410 (2007).
56. Kneipp, K. *et al.* Single molecule detection using surface-enhanced Raman scattering (SERS). *Phys. Rev. Lett.* **78,** 1667–1670 (1997).
57. Michaels, A. M., Jiang, J. & Brus, L. Ag nanocrystal junctions as the site for surface-enhanced Raman scattering of single rhodamine 6G molecules. *J. Phys. Chem. B* **104,** 11965–11971 (2000).
58. Stöckle, R. M., Suh, Y. D., Deckert, V. & Zenobi, R. Nanoscale chemical analysis by tip-enhanced Raman spectroscopy. *Chem. Phys. Lett.* **318,** 131–136 (2000).
59. Anderson, M. S. Locally enhanced Raman spectroscopy with an atomic force microscope. *Appl. Phys. Lett.* **76,** 3130–3132 (2000).
60. Yeo, B. S., Schmid, T., Zhang, W. & Zenobi, R. Towards rapid nanoscale chemical analysis using tip-enhanced Raman spectroscopy with Ag-coated dielectric tips. *Anal. Bioanal. Chem.* **387,** 2655–2662 (2007).
61. Ichimura, T., Hayazawa, N., Hashimoto, M., Inouye, Y. & Kawata, S. Tip-enhanced coherent anti-Stokes Raman scattering for vibrational nanoimaging. *Phys. Rev. Lett.* **92,** 220801 (2004).
62. Hayazawa, N., Motohashi, M., Saito, Y. & Kawata, S. Highly sensitive strain detection in strained silicon by surface-enhanced Raman spectroscopy. *Appl. Phys. Lett.* **86,** 263114 (2005).
63. Lee, N. *et al.* High contrast scanning nano-Raman spectroscopy of silicon. *J. Raman Spectrosc.* **38,** 789–796 (2007).
64. Verma, P., Yamada, K., Watanabe, H., Inouye, Y. & Kawata, S. Near-field Raman scattering investigation of tip effects on C_{60} molecules. *Phys. Rev. B* **73,** 045416 (2006).
65. Domke, K. F., Zhang, D. & Pettinger, B. Tip-enhanced Raman spectra of picomole quantities of DNA nucleobases at Au(111). *J. Am. Chem. Soc.* **129,** 6708–6709 (2007).
66. Rasmussen, A. & Deckert, V. Surface- and tip-enhanced Raman scattering of DNA components. *J. Raman Spectrosc.* **37,** 311–317 (2006).
67. Zhang, W. H., Yeo, B. S., Schmid, T. & Zenobi, R. Single molecule tip-enhanced Raman spectroscopy with silver tips. *J. Phys. Chem. C* **111,** 1733–1738 (2007).
68. Hartschuh, A., Qian, H., Meixner, A. J., Anderson, N. & Novotny, L. Nanoscale optical imaging of single-walled carbon nanotubes. *J. Lumin.* **119–120,** 204–208 (2006).
69. Yano, T., Verma, P., Kawata, S. & Inouye, Y. Diameter-selective near-field Raman analysis and imaging of isolated carbon nanotube bundles. *Appl. Phys. Lett.* **88,** 093125 (2006).
70. Sánchez, E. J., Novotny, L. & Xie, X. S. Near-field fluorescence microscopy based on two-photon excitation with metal tips. *Phys. Rev. Lett.* **82,** 4014–4017 (1999).
71. Yang, H. *et al.* Protein conformational dynamics probed by single-molecule electron transfer. *Science* **302,** 262–266 (2003).
72. Lakowicz, J. R. *et al.* Advances in surface-enhanced fluorescence. *J. Fluoresc.* **14,** 425–441 (2004).
73. Bharadwaj, P., Anger, P. & Novotny, L. Nanoplasmonic enhancement of single-molecule fluorescence. *Nanotechnology* **18,** 44017 (2007).
74. Gerton, J. M. *et al.* Tip-enhanced fluorescence microscopy at 10 nanometer resolution. *Phys. Rev. Lett.* **93,** 180801 (2004).
75. Ma, Z., Gerton, J. M., Wade, L. A. & Quake, S. R. Fluorescence near-field microscopy of DNA at sub-10 nm resolution. *Phys. Rev. Lett.* **97,** 260801 (2006).
76. Huang, F. M., Festy, F. & Richards, D. Tip-enhanced fluorescence imaging of quantum dots. *Appl. Phys. Lett.* **87,** 183101 (2005).
77. Steidtner, J. & Pettinger, B. Tip-enhanced Raman spectroscopy and microscopy on single dye molecules with 15 nm resolution. *Phys. Rev. Lett.* **100,** 236101 (2008).
78. Kühn, S., Håkanson, U., Rogobete, L. & Sandoghdar, V. Enhancement of single-molecule fluorescence using a gold nanoparticle as an optical nanoantenna. *Phys. Rev. Lett.* **97,** 017402 (2006).
79. Hartschuh, A., Qian, H., Meixner, A. J., Anderson, N. & Novotny, L. Nanoscale optical imaging of excitons in single-walled carbon nanotubes. *Nano Lett.* **5,** 2310–2313 (2005).
80. Höppener, C. & Novotny, L. Antenna-based optical imaging of single Ca^{2+} transmembrane proteins in liquids. *Nano Lett.* **8,** 642–646 (2008).
81. Höppener, C. & Novotny, L. Imaging of membrane proteins using antenna-based optical microscopy. *Nanotechnology* **19,** 384012 (2008).
82. Xu, H.-X., Bjerneld, E. J., Käll, M. & Börjesson, L. Spectroscopy of single hemoglobin molecules by surface enhanced Raman scattering. *Phys. Rev. Lett.* **83,** 4357–4360 (1999).
83. Weiβ, J. *et al.* The unimolecular dissociation of the OH stretching states of HOCl: Comparison with experimental data. *J. Chem. Phys.* **115,** 8880–8887 (2001).
84. Hildebrandt, P. & Stockburger, M. Surface-enhanced resonance Raman spectroscopy of rhodamine 6G adsorbed on colloidal silver. *J. Phys. Chem.* **88,** 5935–5944 (1984).
85. Corni, S. & Tomasi, J. Surface enhanced Raman scattering from a single molecule adsorbed on a metal particle aggregate: A theoretical study. *J. Chem. Phys.* **116,** 1156–1164 (2002).
86. Peleg, G. *et al.* Gigantic optical non-linearities from nanoparticle-enhanced molecular probes with potential for selectively imaging the structure and physiology of nanometric regions in cellular systems. *Bioimaging* **4,** 215–324 (1996).
87. Peleg, G., Lewis, A., Linial, M. & Loew, L. M. Nonlinear optical measurement of membrane potential around single molecules at selected cellular sites. *Proc. Natl Acad. Sci. USA* **96,** 6700–6705 (1999).
88. Xu, H., Bjerneld, E. J., Kall, M. & Borjesson, L. Spectroscopy of single hemoglobin molecules by surface enhanced Raman scattering. *Phys. Rev. Lett.* **83,** 4357–4360 (1999).
89. Doering, W. E. & Nie, S. Single-molecule and single-nanoparticle SERS: Examining the roles of surface active sites and chemical enhancement. *J. Phys. Chem. B* **106,** 311–317 (2002).
90. Futamata, M., Maruyama, Y. & Ishikawa, M. Metal nanostructures with single molecule sensitivity in surface enhanced Raman scattering. *Vib. Spectrosc.* **35,** 121–129 (2004).
91. Xu, H. X., Aizpurua, J., Kall, M. & Apell, P. Electromagnetic contributions to single-molecule sensitivity in surface-enhanced Raman scattering. *Phys. Rev. E* **62,** 4318–4324 (2000).
92. Otto, A., Mrozek, I., Grabhorn, H. & Akemann, W. Surface-enhanced Raman scattering. *J. Phys. Condens. Matter* **4,** 1143–1212 (1992).
93. Stöckle, R. M., Deckert, V., Fokas, C., Zeisel, D. & Zenobi, R. Sub-wavelength Raman spectroscopy on isolated silver islands. *Vib. Spectrosc.* **22,** 39–48 (2000).
94. Le Ru, E. C., Meyer, M. & Etchegoin, P. G. Proof of single-molecule sensitivity in surface enhanced Raman scattering (SERS) by means of a two-analyte technique. *J. Phys. Chem. B* **110,** 1944–1948 (2006).
95. Yano, T., Inouye, Y. & Kawata, S. Nanoscale uniaxial pressure effect of a carbon nanotube bundle on tip-enhanced near-field Raman spectra. *Nano Lett.* **6,** 1269–1273 (2006).
96. Bharadwaj, P. & Novotny, L. Spectral dependence of single molecule fluorescence enhancement. *Opt. Express* **15,** 14266–14274 (2007).
97. Ichimura, T. *et al.* Subnanometric near-field Raman investigation in the vicinity of a metallic nanostructure. *Phys. Rev. Lett.* **102,** 186101 (2009).
98. Ichimura, T. *et al.* Temporal fluctuation of tip-enhanced Raman spectra of adenine molecules. *J. Phys. Chem. C* **111,** 9460–9464 (2007).
99. Taguchi, A., Hayazawa, N., Furusawa, K., Ishitobi, H. & Kawata, S. Deep-UV tip-enhanced Raman scattering. *J. Raman Spectrosc.* doi:10.1002/jrs.2287 (2009).
100. Pendry, J. B., Martin-Moreno, L. & Garcia-Vidal, F. J. Mimicking surface plasmons with structured surface. *Science* **305,** 847–848 (2004).

Acknowledgements

This work was supported by the Core Research for Educational Science and Technology (CREST) project of the Japan Science and Technology Corporation, and by the RIKEN Extreme Photonics programme.

Resolution enhancement of a surface immersion microscope near the plasmon resonance

Igor I. Smolyaninov and Christopher C. Davis

Department of Electrical and Computer Engineering, University of Maryland, College Park, Maryland 20742

Jill Elliott and Anatoly V. Zayats

School of Mathematics and Physics, Queen's University of Belfast, Belfast BT7 1NN, United Kingdom

Received March 19, 2004

Resolution of a surface immersion microscope has been studied as a function of surface-plasmon–polariton frequency. Enhancement of resolution near the surface-plasmon resonance has been observed. This effect may potentially be used in direct imaging of biological samples in liquid ambient. © 2005 Optical Society of America

OCIS codes: 180.0180, 240.6680, 240.5420.

Resolution of immersion microscopes[1] is limited by the small range of refractive indices n of available transparent materials. For a while it was believed that the only way to achieve nanometer-scale spatial resolution in an optical microscope is to beat diffraction and detect evanescent optical waves in close proximity to a sample using a near-field optical microscope.[2] However, recently it was realized[3] that a dielectric droplet on a metal surface that supports propagation of surface plasmons[4] may have a large effective refractive index, as seen from these modes. The wave vector of surface plasmons is defined by the expression

$$k_p = \frac{\omega}{c}\left(\frac{\epsilon_d \epsilon_m}{\epsilon_d + \epsilon_m}\right)^{1/2}, \quad (1)$$

where $\epsilon_m(\omega)$ and $\epsilon_d(\omega)$ are the frequency-dependent dielectric constants of the metal and the dielectric. In the vicinity of surface-plasmon resonance defined by

$$\epsilon_m(\omega) = -\epsilon_d(\omega), \quad (2)$$

wavelength λ_p of plasmons becomes small, in other words, the effective refractive index of the dielectric n_{eff} becomes large, as seen by the propagating surface plasmons in this frequency range. As a result, a small droplet of liquid dielectric on the metal surface becomes a strong lens for surface plasmons propagating through the droplet from the outside. On the other hand, the droplet boundary becomes an efficient mirror for surface plasmons propagating inside the droplet at almost any angle of incidence because of total internal reflection. Thus a novel two-dimensional (2D) far-field immersion microscope design (Fig. 1) may be introduced that makes use of the large values of n_{eff} near the plasmon resonance. If a sample under investigation is forced to emit propagating surface plasmons or if it is illuminated by plasmons, these plasmons may produce a 2D magnified image of the sample in the appropriate location on the metal surface that may be subsequently viewed with a regular microscope because of plasmon scattering into photons. Here we describe the operation of such a microscope and study the effect of enhancement of its resolution near the plasmon resonance.

Glycerin microdroplets have been used as 2D optical elements in the design of the microscope. The dielectric constant of glycerin $\epsilon_g = 2.161$ is very close to the real part of the gold dielectric constant $\epsilon_m = -2.256$ (Ref. 5) at the $\lambda_0 = 502$ nm line of an argon-ion laser. According to Eq. (1) the corresponding surface-plasmon wavelength inside glycerin is $\lambda_p = 69.8$ nm, and the effective refractive index of glycerin is $n_{\text{eff}} = \lambda_0/\lambda_p = 7.14$. On the other hand, surface plasmons are not excited at the 458- and 478-nm laser lines. As a result, frequency-dependent anomalously high spatial resolution of the microscope

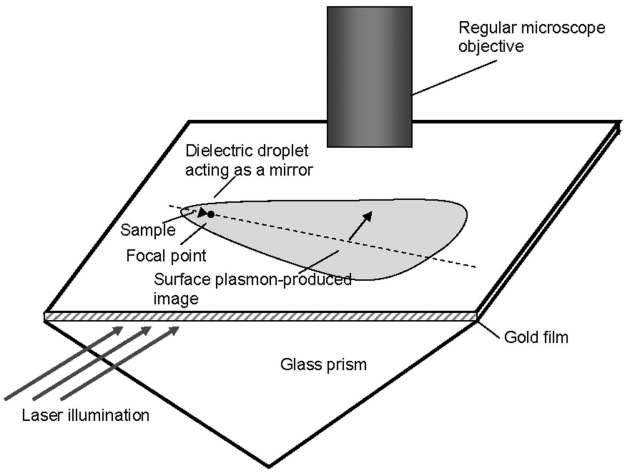

Fig. 1. Geometry of a surface-plasmon immersion microscope. Plasmons are excited by laser light and propagate inside a parabolic-shaped droplet. Placing a sample near the focus of a parabola produces a 2D magnified image in the metal plane, which is viewed from the top by a regular microscope.

0146-9592/05/040382-03$15.00/0

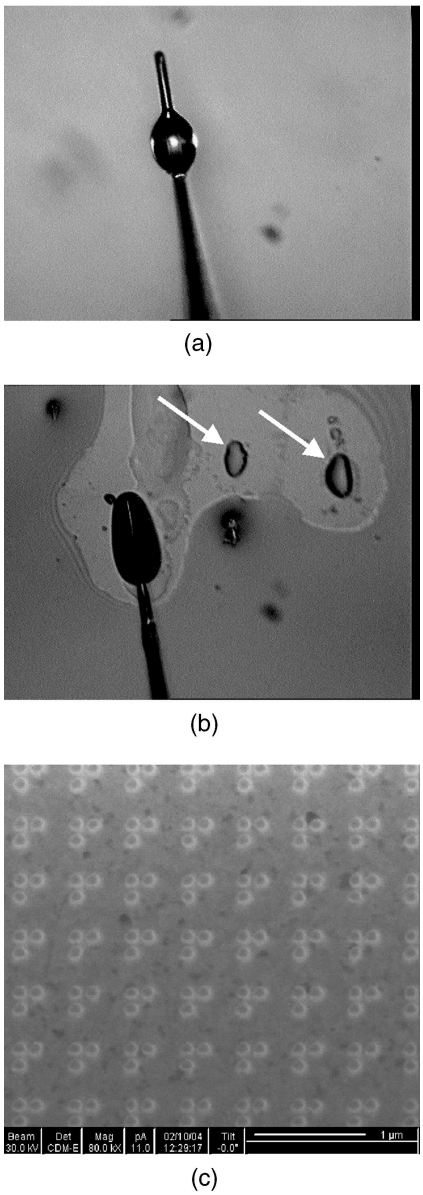

Fig. 2. Glycerin droplets were formed in desired locations by bringing a small probe (a) wetted in glycerin into close proximity to a sample. Bringing the probe to a surface region covered with glycerin led to glycerin microdroplet formation (b) under the probe in locations indicated by the arrows. (c) Electron microscope image of the array of triplet nanoholes used as a test sample.

near 502 nm may be studied. In our experiments the samples were immersed inside glycerin droplets on the gold-film surface. The droplets were formed in desired locations by bringing a small probe [shown in Fig. 2(a)] wetted in glycerin into close proximity to a sample. The probe was prepared from a tapered optical fiber that has an epoxy microdroplet near its apex. Bringing the probe to a surface region covered with glycerin led to glycerin microdroplet formation under the probe [Fig. 2(b)]. The glycerin droplets can be moved to a desired location under visual control by use of a regular microscope. Our droplet deposition procedure allowed us to form droplet shapes that were reasonably close to parabolic. Thus the droplet boundary was used as a 2D parabolic mirror for propagating surface plasmons excited inside the droplet by an external laser. Since the plasmon wavelength is much smaller than the droplet size, the image formation in such a mirror can be analyzed by geometric optics in two dimensions.

Periodic nanohole arrays[6] are ideal test samples for this microscope. When they are illuminated by laser light, such arrays produce propagating surface waves, which explains the anomalous transmission of such arrays at optical frequencies. The frequency-dependent resolution of the microscope was studied with the 30 μm $\times$ 30 μm array of triplet nanoholes (100-nm hole diameter, 40-nm distance between the hole edges) shown in Fig. 2(c). An image of the triplet array obtained at 515 nm is shown in Fig. 3(a) [compare it with theoretical image in Fig. 3(e), calculated with geometric optics, where the droplet shape is also indicated in the figure]. Because of surface roughness and Rayleigh scattering in the dielectric, the propagating plasmons are constantly scattered into normal photons propagating in free

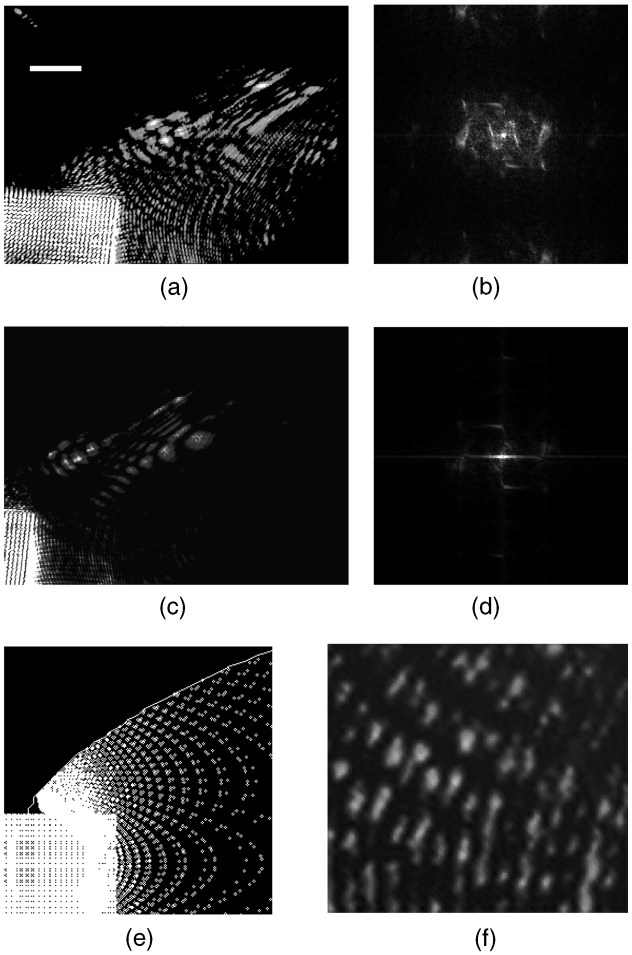

Fig. 3. (a) Image of the triplet nanohole array obtained at 515 nm. The least-distorted part of the image is shown at higher zoom in (f). Comparison of (a) with the theoretically calculated (e) clearly proves the resolving power of the triplet structure. Spatial resolution is lost in (c), taken at 578 nm, which is also confirmed by Fourier analysis of the images in (b) and (d).

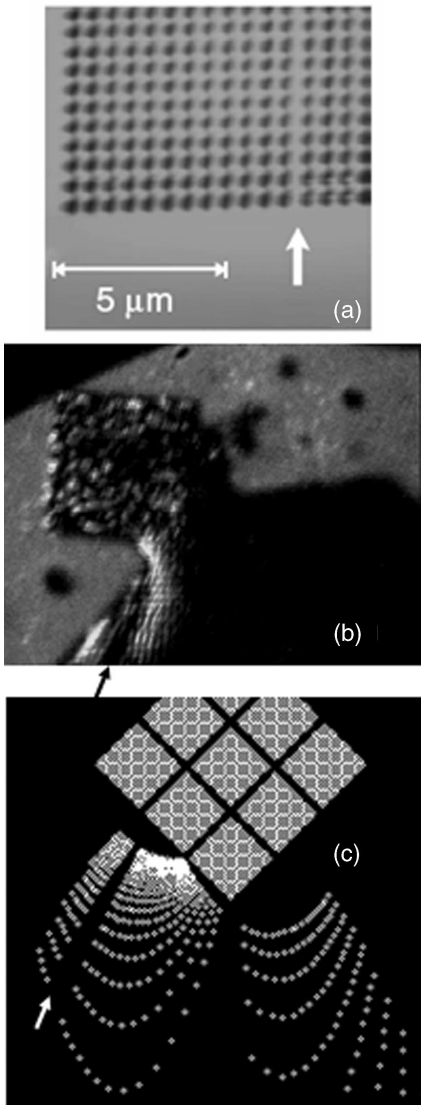

Fig. 4. Images of the gaps in the 30 μm $\times$ 30 μm periodic nanohole array. One of the gaps is indicated by an arrow in (a) the electron microscope image of the structure. Similar gaps are seen in (b) the plasmon microscope image and (c) its theoretical ray-optics reconstruction.

space. As a result, the plasmon-produced far-field 2D image on the metal surface can be visualized by use of a normal optical microscope. The image brightness far exceeds the background of scattered plasmons in other areas of the droplet. The areas of the image close to the droplet edge are distorted, and areas farther from the nanohole array appear to lose resolution because of the limited plasmon propagation length. However, undistorted areas of the image in the vicinity of the nanohole array appear to closely resemble the theoretical image in Fig. 3(e). Each white dot in the theoretical image corresponds to an individual nanohole. The least-distorted part of the image shown at a higher zoom of the conventional optical microscope in Fig. 3(f) presents a clear visualization of the triplet nanohole structure. These triplets of nanoholes are located in close proximity to the focus of the 2D mirror, and hence they experience the highest image magnification. The 40-nm gaps between the nanoholes in the triplets appear to be clearly resolved in most cases. This fact indicates rather high spatial resolution of the microscope. Although it is surprising, this resolution is consistent with the expected $\lambda_p = 69.8$ nm wavelength of surface plasmons excited in the nanohole array sample. The measurements shown in Fig. 3(c), taken at the 478-nm laser line, do not produce a good 2D image of the test structure, which is consistent with the fact that at this frequency surface plasmons are not excited over the gold–glycerin interface. In the immediate vicinity of the nanoholes some periodic image is produced by regular guided modes of the thin glycerin layer. However, Fourier analysis of the images in Figs. 3(a) and 3(c) clearly indicates the loss of spatial resolution away from the plasmon resonance.

Results of experiments performed with other periodic and aperiodic structures can be found in Ref. 7, in which a detailed study of other aspects of image formation is reported. One example of aperiodic sample imaging is presented in Fig. 4. In this figure an image of a gap in a nanohole array was obtained with a surface immersion microscope. The gap width in the image depends linearly on the distance along the optical axis of the 2D imaging system in accordance with the laws of geometric optics.

The plasmon immersion microscope described in this Letter has the potential to become a valuable tool in medical and biological imaging, where far-field optical imaging of individual viruses and DNA molecules may become a reality.

This work was supported in part by National Science Foundation grant 0304046. I. I. Smolyaninov's e-mail address is smoly@eng.umd.edu.

References

1. R. Kingslake, *Optical System Design* (Academic, London, 1983).
2. D. W. Pohl and D. Courjon, *Near Field Optics* (Kluwer Academic, Dordrecht, The Netherlands, 1993).
3. I. I. Smolyaninov, New J. Phys. **5,** 147.1 (2003).
4. H. Raether, *Surface Plasmons* (Springer-Verlag, Berlin, 1988).
5. R. C. Weast, ed., *CRC Handbook of Chemistry and Physics* (CRC Press, Boca Raton, Fla., 1987).
6. T. W. Ebbesen, H. J. Lezec, H. F. Ghaemi, T. Thio, and P. A. Wolff, Nature **391,** 667 (1998).
7. I. I. Smolyaninov, "Far-field optical microscope with nanometer-scale resolution based on in-plane surface plasmon imaging," *arXiv.org e-Print archive*, cond-mat/0405098, May 5, 2004, http://arxiv.org/abs/cond-mat/0405098.